HAL open science

Strigolactones Play an Important Role in Shaping Exodermal Morphology via a KAI2-Dependent Pathway

Guowei Liu, Marina Stirnemann, Christian Gübeli, Susanne Egloff, Pierre-Emmanuel Courty, Sylvain Aubry, Michiel Vandenbussche, Patrice Morel, Didier Reinhardt, Enrico Martinoia, et al.

To cite this version:

Guowei Liu, Marina Stirnemann, Christian Gübeli, Susanne Egloff, Pierre-Emmanuel Courty, et al.. Strigolactones Play an Important Role in Shaping Exodermal Morphology via a KAI2-Dependent Pathway. iScience, 2019, 17, pp.144-154. 10.1016/j.isci.2019.06.024 . hal-02389739

HAL Id: hal-02389739

https://hal.science/hal-02389739

Submitted on 26 May 2020

HAL is a multi-disciplinary open access archive for the deposit and dissemination of scientific research documents, whether they are published or not. The documents may come from teaching and research institutions in France or abroad, or from public or private research centers.

L'archive ouverte pluridisciplinaire **HAL**, est destinée au dépôt et à la diffusion de documents scientifiques de niveau recherche, publiés ou non, émanant des établissements d'enseignement et de recherche français ou étrangers, des laboratoires publics ou privés.

Distributed under a Creative Commons Attribution - NonCommercial - NoDerivatives 4.0 International License

iScience

CellPress

Article

Strigolactones Play an Important Role in Shaping Exodermal Morphology via a KAI2-Dependent Pathway

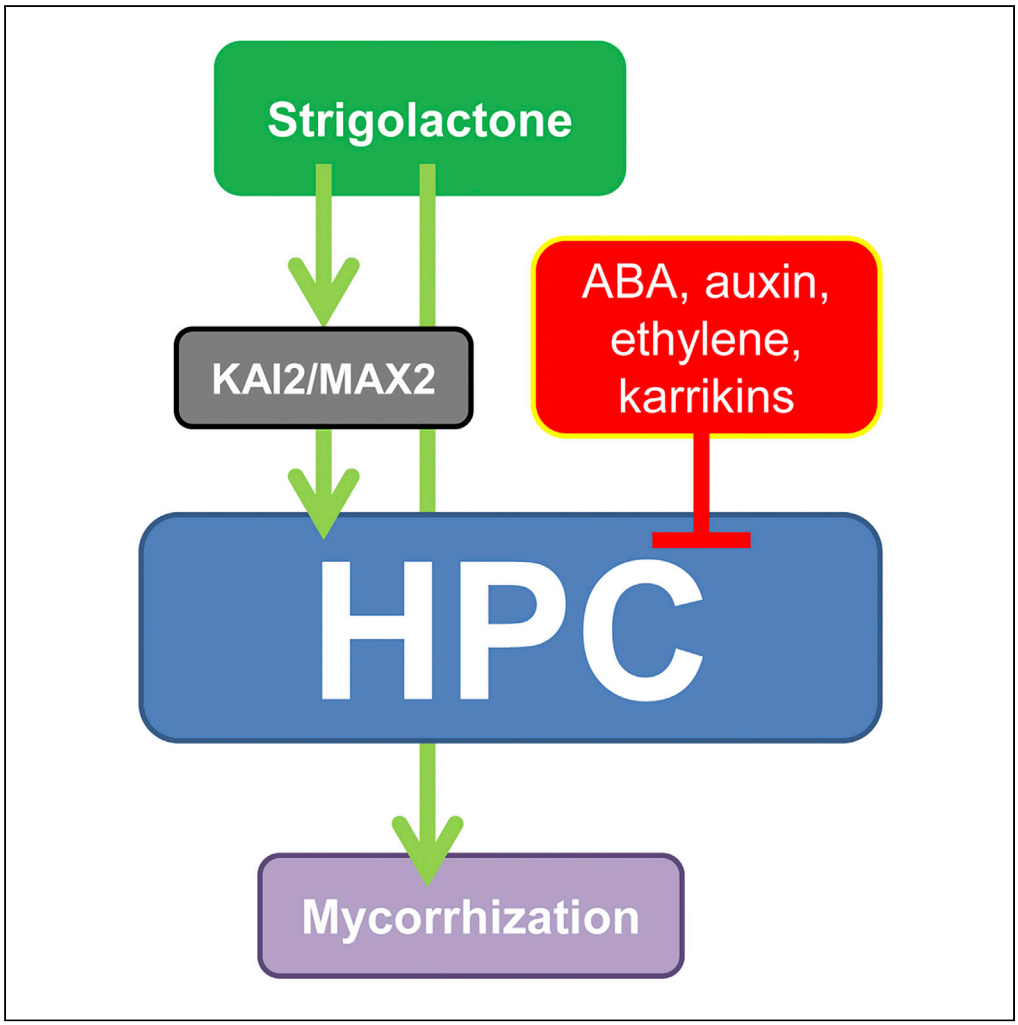

Guowei Liu, Marina Stirnemann, Christian Gübeli, ..., Didier Reinhardt, Enrico Martinoia, Lorenzo Borghi

enrico.martinoia@uzh.ch (E.M.)
lorenzo.borghi@uzh.zh (L.B.)

HIGHLIGHTS

Strigolactones induce the presence of hypodermal passage cells (HPC) in the root

ABA, ethylene, auxin, and karrikins negatively regulate the density of HPC

HPC density is regulated by the KAI2/MAX2 signaling pathway

Hormonal cross talk regulates HPC density and therefore hypodermis permeability

Liu et al., iScience *17*, 144–154
July 26, 2019 © 2019 The Authors.
https://doi.org/10.1016/j.isci.2019.06.024

iScience

CellPress

Article

Strigolactones Play an Important Role in Shaping Exodermal Morphology via a KAI2-Dependent Pathway

Guowei Liu,[1] Marina Stirnemann,[1] Christian Gübeli,[1] Susanne Egloff,[1] Pierre-Emmanuel Courty,[2] Sylvain Aubry,[1] Michiel Vandenbussche,[3] Patrice Morel,[3] Didier Reinhardt,[4] Enrico Martinoia,[1,*] and Lorenzo Borghi[1,5,*]

SUMMARY

The majority of land plants have two suberized root barriers: the endodermis and the hypodermis (exodermis). Both barriers bear non-suberized passage cells that are thought to regulate water and nutrient exchange between the root and the soil. We learned a lot about endodermal passage cells, whereas our knowledge on hypodermal passage cells (HPCs) is still very scarce. Here we report on factors regulating the HPC number in Petunia roots. Strigolactones exhibit a positive effect, whereas supply of abscisic acid (ABA), ethylene, and auxin result in a strong reduction of the HPC number. Unexpectedly the strigolactone signaling mutant d14/*dad2* showed significantly higher HPC numbers than the wild-type. In contrast, its mutant counterpart *max2* of the heterodimeric receptor DAD2/MAX2 displayed a significant decrease in HPC number. A mutation in the Petunia karrikin sensor KAI2 exhibits drastically decreased HPC amounts, supporting the hypothesis that the dimeric KAI2/MAX2 receptor is central in determining the HPC number.

INTRODUCTION

Many plant roots possess two barrier layers, the exodermis (or hypodermis) and endodermis (Sharda and Koide, 2008; Rich et al., 2014). Both layers consist of a sheet of cells with suberin-coated (suberized) impermeable cell walls, but they also contain a limited number of non-suberized "passage cells", which allow the passage of liquids and solutes. However, the passage cells from exodermis and endodermis differ in several structural and functional aspects (Peterson and Enstone, 1996). The inner layer, the endodermis, is structurally very similar in most plants, and only few are known to lack an endodermis (Enstone et al., 2002). The cells of the endodermis are surrounded by the Casparian strips that block the apoplastic passage between cells, thereby acting as a barrier between the cortex and the stele, and restricting ion transport to trans-cellular transport across the endodermis. Rare non-suberized endodermal cells, so called endodermal passage cells, facilitate transport across the endodermis and act as important players for ion sequestration in the stele (Barberon et al., 2016). Recent work showed that endodermal passage cells are localized close to the xylem (Andersen et al., 2018), and it was suggested that hormonal signaling from the vasculature promotes their differentiation. Similar to the endodermis, the hypodermis contains non-suberized hypodermal passage cells (HPCs) that are thought to facilitate the uptake of nutrients into the cortex. A hypodermal layer occurs in the majority of land plants, including many staple food crops (Shishkoff, 1987).

Significant progress has been made in our understanding of the differentiation of the endodermis and its passage cells (Barberon et al., 2016; Doblas et al., 2017; Andersen et al., 2018); however, much less is known about the formation of the hypodermis and the HPCs. Early work showed that the degree of HPC suberization increases when plants suffer water stress and that the increased suberization protects plants from water loss (Hose et al., 2001). In addition to their suspected role in facilitating nutrient transfer, HPCs are shown to serve as gateways for arbuscular mycorrhizal fungi (Sharda and Koide, 2008), which establish a symbiosis that allows plants to efficiently scavenge for mineral nutrients such as phosphate. HPCs express the ABCG protein PLEIOTROPIC DRUG RESISTANCE 1 (PDR1), which is localized to the plasma membrane (Kretzschmar et al., 2012; Sasse et al., 2015) and mediates secretion of the phytohormone strigolactones (SLs) that promote mycorrhization by inducing fungal hyphal branching (Parniske, 2008; Al-Babili and Bouwmeester, 2015).

Increased expression of PDR1 results in higher SL secretion (Sasse et al., 2015) and stronger mycorrhizal colonization (Liu et al., 2018a, 2018b). In contrast, *pdr1 ko* mutants exude very low amounts of SL and

[1]Department of Plant and Microbial Biology, University of Zurich, 8008 Zurich, Switzerland

[2]Laboratoire Reproduction et Développement des Plantes, Univ Lyon, ENS de Lyon, UCB Lyon 1, CNRS, INRA, 69342 Lyon, France

[3]Department of Reproduction and Plant Development, CNRS/INRA/ENS, 69634 Lyon, France

[4]Department of Biology, University of Fribourg, 1700 Fribourg, Switzerland

[5]Lead Contact

*Correspondence: enrico.martinoia@uzh.ch (E.M.), lorenzo.borghi@uzh.zh (L.B.)

https://doi.org/10.1016/j.isci.2019.06.024

 © 2019 The Authors.
This is an open access article under the CC BY-NC-ND license (http://creativecommons.org/licenses/by-nc-nd/4.0/).

exhibit decreased mycorrhizal colonization rates nearly similar to the SL biosynthetic mutant *dad1* (Kretzschmar et al., 2012). Based on this collective evidence, we investigated whether PDR1 or SLs play a role on the presence of HPC.

RESULTS

HPCs are non-suberized cells of the hypodermis, i.e., they are located just beneath the thin, non-suberized epidermis. The method of choice to identify HPCs is trypan blue staining, as already reported in several publications (Figures 1A–1I, see Transparent Methods and Table S1) (Shishkoff, 1987; Peterson and Enstone, 1996; Kretzschmar et al., 2012). A protocol based on fluorol yellow, previously used for endodermal passage cell quantification in *Arabidopsis*, could not be applied because of hypodermal auto-fluorescence in *Petunia* (Figures S1A–S1D). First, we determined the numbers of HPCs in *pdr1* and *dad1* mutant lines and their corresponding wild-type (WT) backgrounds. Both *pdr1* and *dad1* mutants exhibited only about half the HPC density (HPCs/cm of root) in their primary root compared to the WT (Figures 1J and 1K, black bars). HPCs were quantified (1) per centimeter of root length (Figures S1E and S1F), (2) per total root length, and (3) as a fraction of all hypodermal cells (‰) (Transparent Methods) (Figures S2A–S2E). The latter ways of quantification allowed us to normalize HPC density for root length in centimeters and cell number, respectively (Figures S2F and S2G). Altogether, these results show that plants defective in SL biosynthesis or secretion have fewer HPCs. The fact that HPC density was fully restored in *dad1* and *pdr1* mutants by the addition of *rac-GR24*, a synthetic SL analogue, shows that HPC presence is stimulated by SL (Figures 1J and 1K, gray bars).

The HPC density in roots was shown to decrease over time (Sharda and Koide, 2008), presumably as a result of gradually increasing suberin deposition in hypodermal cells. This results in a developmental gradient with the highest HPC density at the root tip and decreasing density along the proximal parts of the root (Figures S1E and S1F). To assess the dynamics of HPC density, we performed a time course experiment over 6 weeks of root development. The HPC density decreased in the WT (V26) from an initial 13 HPC/cm root to less than 5, whereas *dad1* had <5 HPC/cm root length at all times (Figure 1L). Similar, albeit less significant, results were obtained with lateral roots (Figure 1M).

SLs are part of a complex hormonal regulatory network that also involves auxin, ABA, and ethylene (Hayward et al., 2009; Lopez-Raez et al., 2010; Ueda and Kusaba, 2015); hence, we investigated the impact of these hormones on HPC differentiation. ABA is known to promote suberization of plant tissues (Leide et al., 2012; Boher et al., 2013; Ueda and Kusaba, 2015), and, in line with this function, exogenous ABA application decreased the density of HPCs in WT *Petunia* roots as well as in *pdr1* and *dad1* mutants (Figure 2A). *DAD1* and *PDR1* are involved in SL biosynthesis and exudation, respectively (Kretzschmar et al., 2012). *PDR1* is induced by SL, whereas *DAD1* is subject to negative feedback regulation by SL (Sasse et al., 2015). We quantified *PDR1* and *DAD1* expression levels after treatments with *rac-GR24* and ABA. In both WT backgrounds (W115XW138 and V26) *PDR1* was upregulated by *rac*-GR24 and downregulated by ABA, whereas *DAD1* was downregulated by both *rac-GR24* and ABA (Figures S3A and S3B).

Ethylene is an established negative regulator of mycorrhizal development (Martín Rodriguez et al., 2010). To test the effect of ethylene on HPC density, we treated *Petunia* seedlings either with the ethylene precursor ACC (aminocyclopropane-1-carboxylic acid) or the ethylene releaser ethephon. This allowed us to increase endogenous ethylene production (from ACC) and exogenous ethylene exposure (from ethephon). Both treatments strongly reduced the density of HPCs in three WT backgrounds (Figure 2B). This result is consistent with the reported negative effect of ethylene on plant mycorrhization (Varma Penmetsa et al., 2008).

Previous studies have shown that *PDR1*, as well as the SL biosynthesis genes *CAROTENOID CLEAVAGE DEOXYGENASE7 (CCD7)/RAMOSUS5* and *CCD8/RAMOSUS1*, is upregulated by auxin (Hayward et al., 2009; Kretzschmar et al., 2012). Thus, auxin could potentially increase HPC density through increased SL biosynthesis and secretion. In contrast, however, the auxin NAA caused strongly reduced HPC densities at concentrations of 1 μM (Figure 2C) or 100 nM NAA (Figure S3C). Auxin can induce ethylene biosynthesis; hence, the reduction of HPC density by auxin could potentially be caused by increased ethylene levels (Hansen and Grossmann, 2000). However, addition of the ethylene antagonist AVG (amino-ethoxy-vinylglycine) to the medium did not reverse the decrease in HPC density caused by auxin (Figure 2C), indicating that the reduction of HPC density by auxin does not involve ethylene. We further tested the effect of auxin on HPC presence using transgenic petunia lines that express *p35CaMVS:indoleacetic acid-lysine*

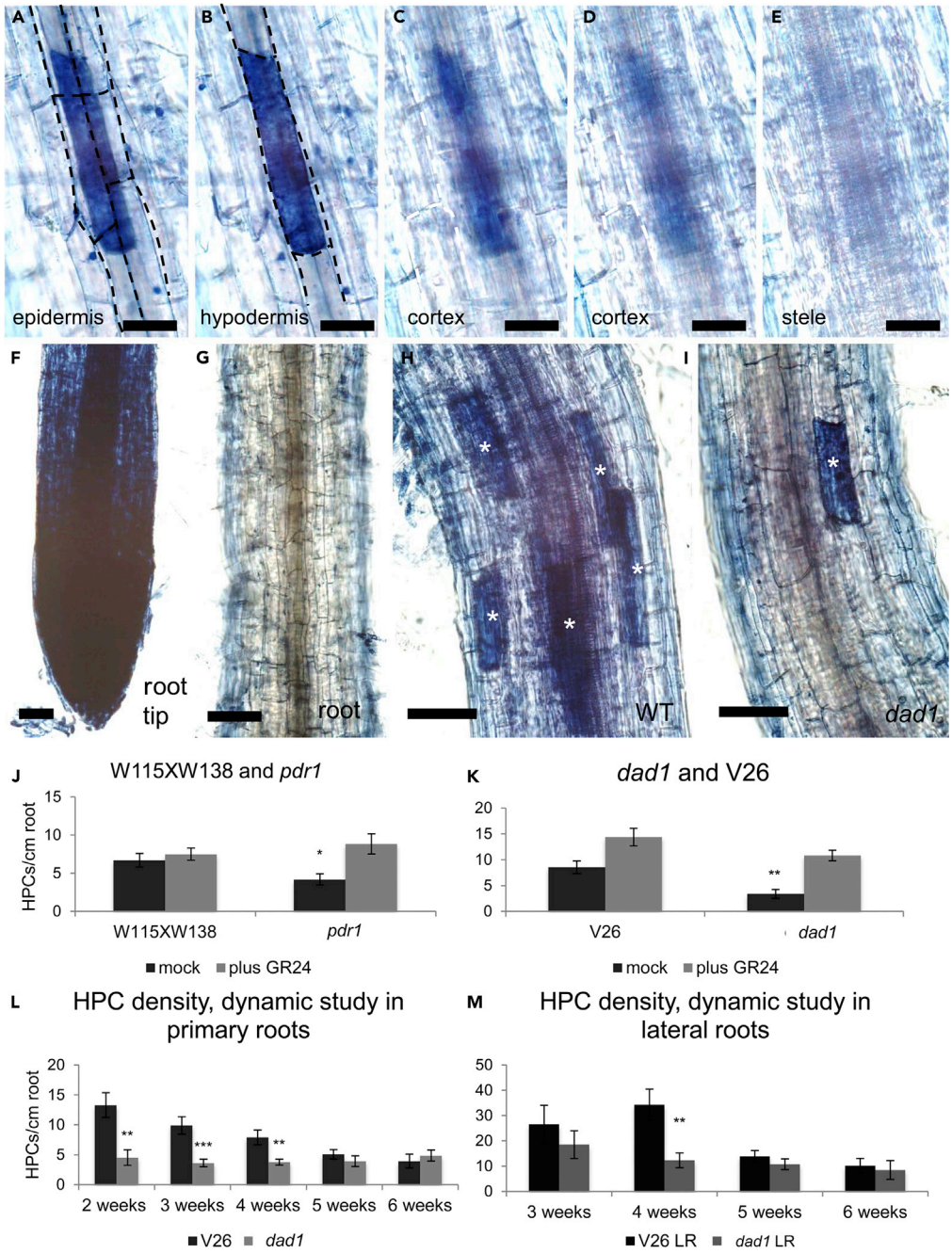

Figure 1. Effect of Strigolactones (SL) on Hypodermal Passage Cell Density

(A–I) Trypan-blue-stained HPCs. Top view on the epidermal layer (A), hypodermis (B), inner cortex layer one (C), inner cortex layer two (D), and stele (E). Root tip from primary root (F), differentiated cells in root segment 7 cm above the root tip (G), representative HPCs in WT (H), and in *dad1* (I).

(J and K) HPC density in the SL transporter mutant *pdr1* and in the SL biosynthesis mutant *dad1*; the density of HPCs in the SL biosynthesis mutant *dad1* can be restored by exogenous 10 μM GR24.

(L and M) HPC density dynamics in primary and lateral roots of V26 and *dad1* mutant. HPC density was quantified in 2-, 3-, 4-, 5-, and 6-week-old seedlings.

Stars above the bars indicate statistically significant difference (t test, *$p \leq 0.05$, **$p \leq 0.01$, ***$p \leq 0.001$). For clear view of data, scales in Figures 1J–1M are different. Scale bar, 50 μM (A–E, H, and I) and 250 μM (F and G). Error bars are ±SEM.

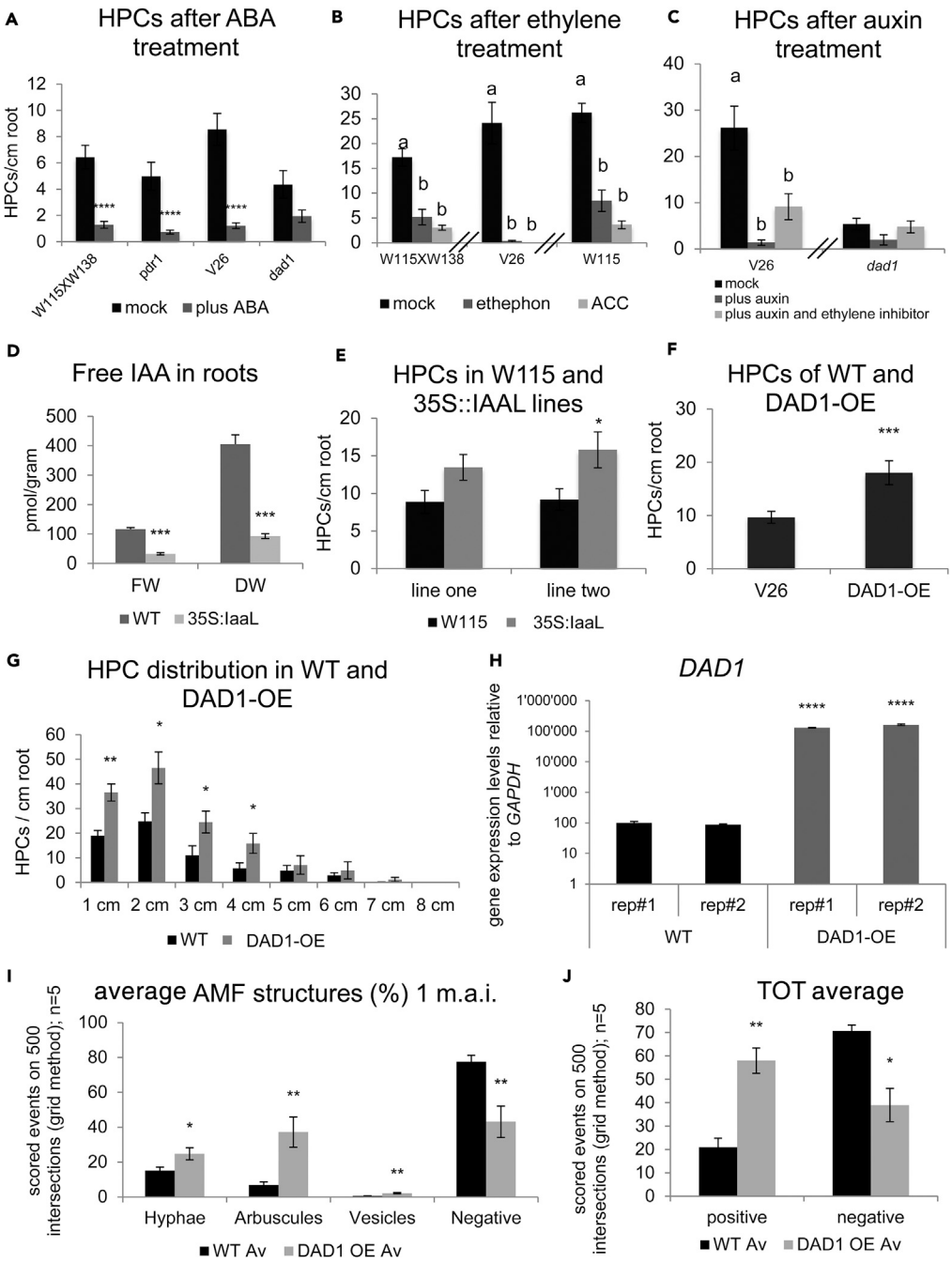

Figure 2. Exogenous Hormonal Treatments Affect HPCs Density

(A) Effect of 1 μM ABA on HPC density.

(B) Effect of ethylene on HPC density (1 μM ethephone or 5 μM ACC).

(C) Effect of 1 μM Auxin (NAA) and 10 μM AVG on HPC density.

(D) Free auxin content in WT and 35S:IaaL lines expressed relative to both fresh weight (FW) and dry weight (DW).

(E) HPC densities in *Petunia* plants transgenic for the over-expression of the auxin-lysine conjugation enzyme (35S:IaaL).

(F) HPC density in V26 and DAD1-OE roots.

(G) HPC distribution in WT and DAD1-OE lines.

(H) *DAD1* expression in WT and DAD1-OE lines.

(I) Arbuscular mycorrhizal (AM) structures quantified in WT and DAD1-OE roots 1 month after inoculation (m.a.i.) with *Rhizophagus irregularis*: hyphae, intraradical arbuscules, and vesicles. Negative means no AM structure detected.

(J) Mycorrhization rates in W115 and DAD1-OE.

Figure 2. *Continued*

Different letters above the bars indicate statistically significant difference ($p < 0.05$, by one-way ANOVA, $n \geq 30$). Stars above the bars indicate statistically significant difference (t test, $^{*}p \leq 0.05$, $^{**}p \leq 0.01$, $^{***}p \leq 0.001$, $^{****}p \leq 0.0001$). Error bars are ±SEM. See Table S1.

synthetase (35S:IaaL). IaaL conjugates IAA to lysine, thereby depleting endogenous free IAA pools (Romano et al., 1991). Indeed, IaaL expression reduced free IAA levels in petunia (Figure 2D), and these plants exhibited an increased HPC density relative to WT plants (Figure 2E), consistent with a negative effect of auxin on HPC presence.

The central enzyme in SL biosynthesis is CCD8, which catalyzes a series of reactions resulting in the formation of the SL precursor carlactone (Seto et al., 2019). Transgenic petunia plants overexpressing DAD1/CCD8 (DAD1-OE) exhibited nearly double the HPC density of the WT (Figure 2F); thus, the presence of HPCs is stimulated by high levels of *DAD1* expression (Figures 2G and 2H). We also observed that DAD1-OE plants showed significantly higher levels of mycorrhizal colonization compared with the WT (Figures 2I and 2J). These results show that *DAD1* overexpression increases HPC density and promotes arbuscular mycorrhizal (AM) symbiosis.

To assess the dependency of HPC presence on SL signaling, we tested whether HPC density was affected in *dad2* and *max2a* mutants. DAD2 is part of the heterodimeric SL receptor complex and bears the α/β hydrolase activity required for SL signal transduction (Drummond et al., 2011). The other partner is MAX2A (Drummond et al., 2011), an F box protein homologous to AtMAX2, which interacts with DAD2 in the presence of GR24 resulting in SL signaling (in contrast to its close homologue MAX2B, which is not involved in SL signaling) (Hamiaux et al., 2012). Surprisingly, HPC density was significantly increased in *dad2* mutants compared with the WT (V26) (Figure 3A). Since exogenous SL induced the number of HPCs (Figures 1J and 1K), we suspected that increased HPC density in *dad2* might be caused by a compensatory stimulation of SL biosynthesis. Consistent with this hypothesis, *DAD1* expression was considerably increased in *dad2* compared with V26 (Figure 3B), and the levels of mycorrhizal colonization were significantly higher (Figure 3C). In conjunction with our overexpression data (Figures 2I and 2J), this indicates that increased *DAD1* expression levels in *dad2* may be sufficient to increase HPC density and stimulate AM development.

In contrast to *dad2*, *max2a* mutants (Figures S3D and S3E) showed a pronounced decrease in HPC number compared with the corresponding WT (W115XW138) (Figure 3D). Expression of the SL biosynthesis genes *DAD1* and *MAX1* was not significantly affected in *max2a* mutants (Figure 3E). The contrasting HPC densities of the two supposed SL signaling mutants *dad2* and *max2a* could be related to their interaction partners. In *Arabidopsis*, MAX2 is involved not only in SL perception (complex of DAD2 and MAX2) but also in karrikin (KAR) perception, which is mediated through the KARRIKIN INSENSITIVE 2 (KAI2)/MAX2 heterodimeric receptor complex (Marzec, 2016).

To test whether *KAI2* may have a function in the regulation of HPC density, we sought for a *kai2* mutant in *Petunia*. In contrast to the single-copy genes *DAD1*, *MAX2A* (*MAX2B* is not involved in SL signaling), and *PDR1* (Snowden et al., 2005; Drummond et al., 2011; Kretzschmar et al., 2012), the petunia genome contains five closely related *KAI2* homologues (*KAI2a-e*) (Figure S4A). To assess which of them might have a role in AM, their expression pattern was determined, and only *KAI2a* was found to be expressed in roots at detectable levels (Figure S4B). Two independent *kai2a* mutant alleles showed enlarged leaf blades (Figures S4C–S4E), as in the case of *Arabidopsis kai2* mutants (Bennett et al., 2016). Quantification of HPCs revealed dramatically reduced HPC densities in both lines compared with the corresponding WT background W138 (Figure 3F). Remarkably, *kai2a* mutants were entirely resistant to AM infection (Figure S3F). A similar AM-defective mutant phenotype was recently shown in rice *kai2* mutants (Gutjahr et al., 2015). These results suggest that HPC density might rely on a KAI2/MAX2-dependent signaling pathway.

To test whether karrikins may have a role in HPC density, we treated WT and *max2a* mutants with karrikin1 and karrikin2, two established substrates of KAI2 in *Arabidopsis* (Conn and Nelson, 2016), at concentrations from 10 nM to 1 μM. Unexpectedly, karrikins reduced HPC density in WT plants (Figures 4A and S3C), whereas HPC density in *max2a* mutants was not affected by karrikins. This indicates that the repressive effect of karrikins on HPCs requires MAX2. Based on these results, we hypothesize that karrikins might downregulate *DAD1* expression levels in a MAX2-dependent manner, as reported in Arabidopsis (Nelson et al., 2011), and/or that they may compete with a yet unknown KAI2a ligand (KAI2a-L) that acts as a positive regulator of HPC presence in *Petunia*. Indeed, karrikin treatments strongly reduced *DAD1* expression (Figure S3G).

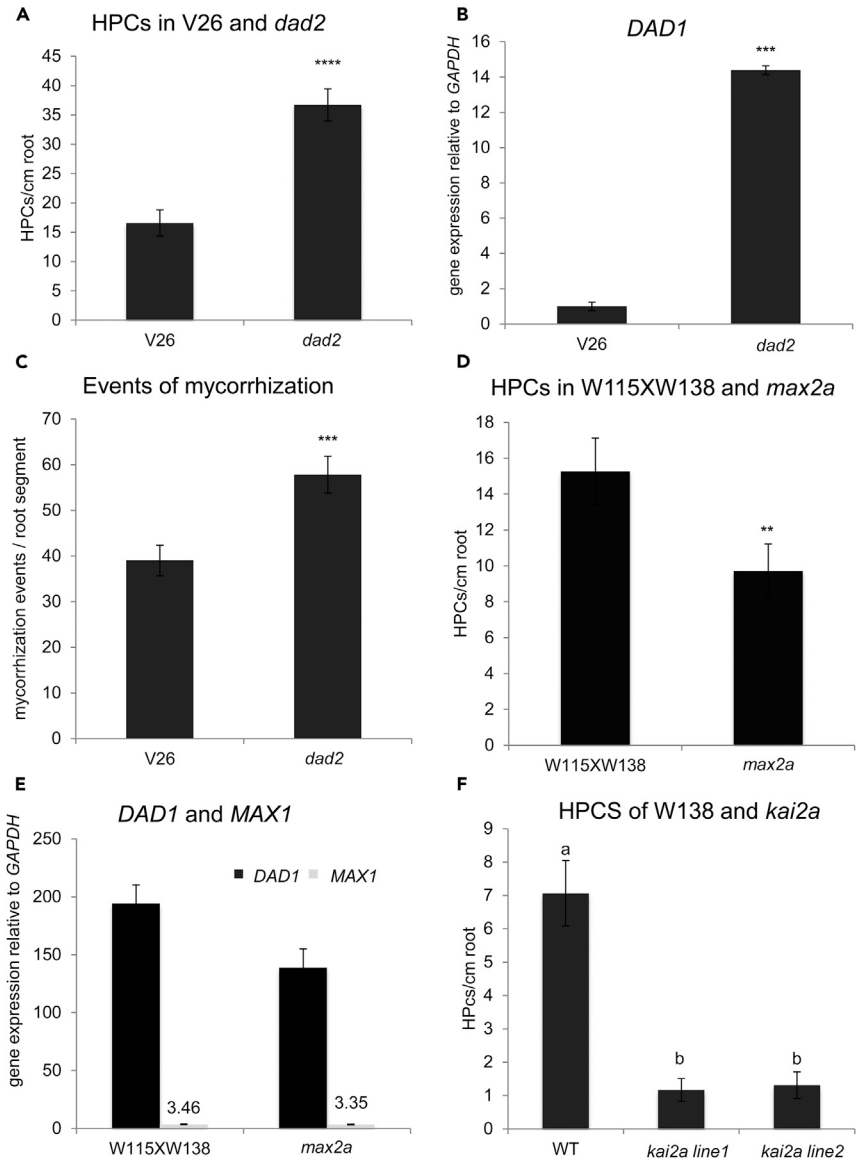

Figure 3. Presence of HPCs is MAX2-Dependent and DAD2-Independent

(A) HPC density in *dad2* and WT roots.

(B) *DAD1* expression in *dad2* mutant.

(C) Mycorrhization ratios in V26 and *dad2* mutant.

(D) HPC density in *max2a*.

(E) *DAD1* and *MAX1* gene expression levels in *max2a*.

(F) HPC density in *kai2a*.

Different letters above the bars indicate statistically significant difference ($p < 0.05$, by one-way ANOVA, $n \geq 30$). Stars above the bars indicate statistically significant difference (t test, $*p \leq 0.05$, $**p \leq 0.01$, $***p \leq 0.001$, $****p \leq 0.0001$). Error bars are $\pm$SEM. See Table S1.

Arabidopsis KAI2 was shown to bind karrikins, GR24, and a related class of small molecules (cotylimides). In addition, GR24 and cotylimides promote the dimerization of MAX2 and KAI2 in yeast, implicating that they could potentially trigger KAI2-dependent signaling (Toh et al., 2014). Based on this evidence, we tested whether the enantiomers contained in rac-GR24 may promote HPC presence in a KAI2-dependent fashion. Indeed, we found that $GR24^{5DS}$ but not $GR24^{ent\text{-}5DS}$ increased the number of HPCs in WT plants but not in *kai2a* mutants (Figure 4B). $GR24^{5DS}$ also increased HPC density in *dad1* mutants (Figure 4C) as did rac-GR24

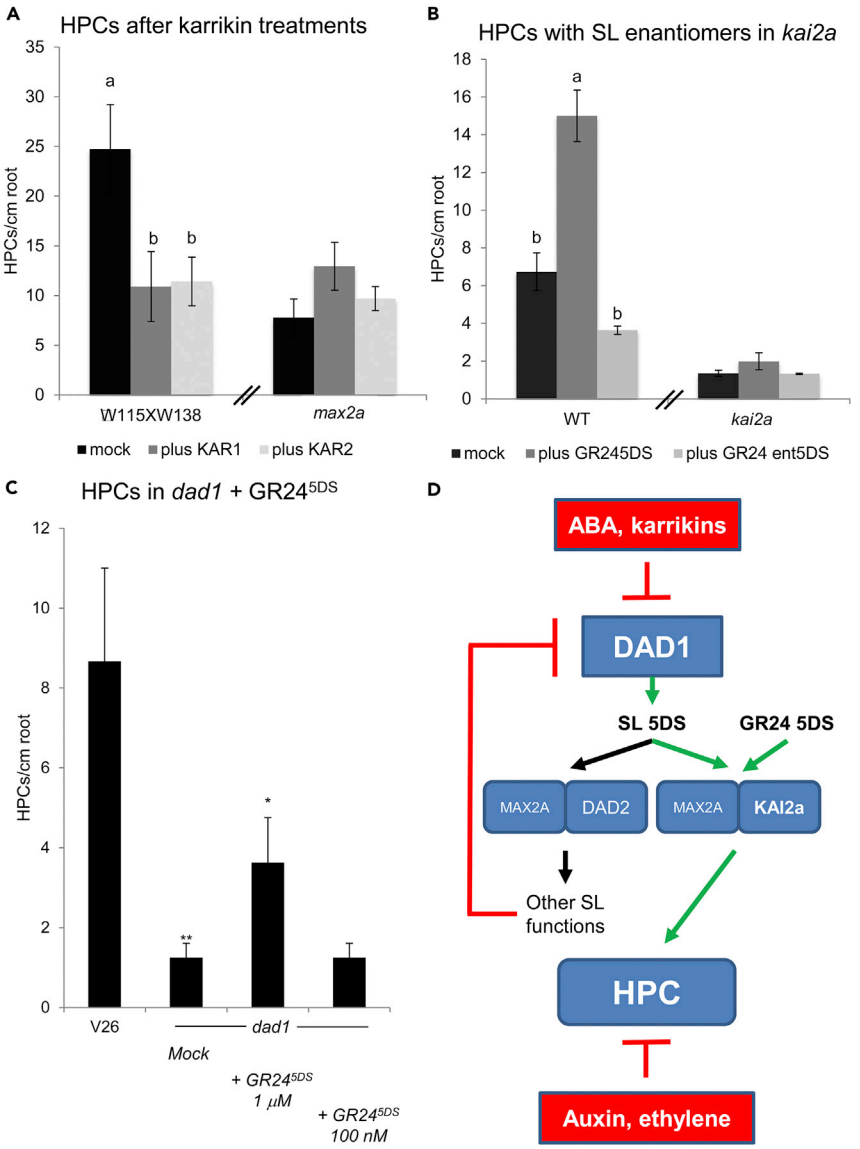

Figure 4. Effects of GR24 Enantiomers and Karrikins on HPCs

(A) HPC density after 1 μM karrikin1 and 1 μM karrikin2 treatments.

(B) HPC density in WT and *kai2a* after treatments with 1 μM GR24 enantiomers.

(C) HPCs in *dad1* after treatments with mock, 1 μM, and 100 nM $GR24^{5DS}$.

(D) Model of HPC regulation via SL^{5DS}.

Different letters above the bars indicate statistically significant difference ($p < 0.05$, by one-way ANOVA, $n \geq 30$). When no letters, no significant difference. Stars above the bars indicate statistically significant difference (Student's t test p value < 0.05 = *; <0.001 = **). Error bars are ±SEM. See Table S1.

(Figure S2A). Taken together, these results suggest that KAI2a promotes HPC presence involving a DAD1-derivative that is transported by PDR1 and that has features of a canonical 5DS strigolactone (Figure 4D).

DISCUSSION

HPCs are a characteristic feature of the roots in many plants, and they are relevant for water flux control (Steudle, 2000) and fungal infection in AM symbiosis. Hence, HPC density is an important determinant of plant fitness, and therefore it can be expected to be under tight developmental and environmental

control. Here, we show that HPC density is subject to hormonal regulation. SLs promoted HPC presence, whereas ABA, auxin, ethylene, and karrikins reduced HPC density.

The negative hormonal effects of ABA, auxin, and ethylene on HPC density relate to a large body of published knowledge and open interesting new avenues of research. The ABA effect is consistent with the reported function of this hormone in root suberization induced by drought stress (Christmann et al., 2007; Charpentier et al., 2014) and in the induction of scar tissue suberization in tomato fruits (Christmann et al., 2007; Leide et al., 2012). However, the function of ABA in AM is complex, since certain levels of ABA are required for symbiotic development (Charpentier et al., 2014), whereas high concentrations inhibit AM. Although several papers reported a cross talk between ABA and SL (Tsuchiya and McCourt, 2009; Conn and Nelson, 2016), the interaction between these two hormones remains elusive, except for the fact that abiotic stresses can shift the balance between their syntheses toward ABA, which may involve competition for common precursors (Liu et al., 2015).

Effects of ethylene and auxin have also been documented for the formation of passage cells in the endodermis of *Arabidopsis* (Barberon et al., 2016), but in these cases, the hormones promoted passage cell formation instead of reducing their density as in our study. Whether this reflects differences between the species or rather between the tissue layers (endodermis vs. hypodermis) remains to be investigated. A possible function of ethylene in controlling hypodermal passage cell number is suggested by the observation that ethylene application significantly increased the concentration of ABA in rice roots (Ma et al., 2014), which indicates that ethylene might regulate the presence of HPCs through ABA.

The promotive effect of SL on HPC density, and the fact that only the 5DS enantiomer was active, prompted us to further explore this phenomenon with transposon-generated loss-of-function mutants in signaling genes *MAX2A*, *DAD2*, and *KAI2a* and in the SL biosynthetic gene *DAD1*. *MAX2A* and *DAD2* have previously been shown to encode components of the SL receptor (Drummond et al., 2011). As expected, *max2a* mutants showed the bushy phenotype known from previously described *MAX2a* knockdown lines in *Petunia* (Drummond et al., 2011) and from mutants in *Arabidopsis* (Stirnberg et al., 2002).

Unexpectedly, however, *dad2* and *max2a* showed opposite phenotypes regarding HPC density, with decreased density in *max2a* and increased density in *dad2*. Increased HPC density in *dad2*, and a concomitant increase in AM colonization, can be explained with increased SL biosynthesis, since *DAD1* was upregulated in *dad2* (Figure 3B), and DAD1-OE showed a similar phenotype (Figures 2H–2J). These results also implicate that the promotion of HPC density by SL acts independently of *DAD2*, whereas *MAX2A* is required. It is interesting to note that the symbiotic phenotypes of mutants in the *DAD2* and *MAX2a* orthologues in rice, DWARF14 (D14) and DWARF3 (D3), respectively, were similar as in petunia: *d14* mutants showed higher AM colonization, whereas *d3* mutants exhibited reduced AM colonization (Yoshida et al., 2012). It remains to be seen whether the contrasting AM colonization phenotypes in these rice mutants correlate with HPC densities.

The fact that HPC density was reduced in *max2* but not in *dad2* hints to an SL-related perception mechanism that involves MAX2A in conjunction with another protein partner than DAD2. MAX2 has alternative interaction partners such as KAI2 to form receptor complexes that can perceive molecules such as not only karrikins (Scaffidi et al., 2014) but also SLs and a predicted, so far unidentified endogenous hormonal KAI2 ligand (Nelson et al., 2011). *Petunia* has five *KAI2* homologues of which only one, *KAI2a*, is expressed in roots. *Kai2a* mutants had an equally strong HPC phenotype as the SL-defective *dad1* mutant, suggesting that KAI2a may act as a non-redundant receptor for a DAD1-derived 5DS putative strigolactone signal that promotes HPC differentiation.

The fact that *kai2a* mutants exhibited strongly reduced HPC densities suggests the involvement of a positively acting KAI2a ligand. However, the reported KAI2 ligands, karrikins, reduced HPC numbers. Karrikins as exogenous growth regulators may interfere with HPC formation through KAI2 signaling by competing with an endogenous positive regulator (e.g., an elusive KAI2 ligand). The fact that the SL analogue GR24 only acted in its 5DS form and that this effect disappeared in *kai2a* mutants indicates that a *bona fide* receptor system mediates the SL-dependent promotion of HPC presence, and based on our data, we propose that it involves KAI2a/MAX2A. In this context, it is interesting to note that *kai2* mutants in rice exhibit strongly reduced mycorrhizal colonization (Gutjahr et al., 2015). Thus, it would be informative to test whether *kai2* rice mutants are affected in HPC density.

In summary, HPC density in *Petunia* roots depends on SL and its transport via PDR1. In particular, the SL^{5DS} enantiomer promoted HPC density through a MAX2/KAI2a-dependent signaling pathway. These results for the first time associate the KAI2 signaling pathway to the presence of a specific cell type, the HPCs. We show here that *Petunia* plants with high expression levels of *DAD1*, either in *dad2* loss-of-function mutants or DAD1 OE lines, have increased HPC density compared with WT. Thus, not only exogenous application of $GR24^{5DS}$ but also genetic approaches to increase endogenous SL biosynthesis positively affected HPC density. Consistent with these findings, treatments with hormones and molecules that decreased *DAD1* gene expression, e.g., ABA and karrikins, reduced HPC density. In addition, auxin and ethylene independently reduced HPC density, via yet unknown pathways. Increased HPC density in *dad2* and DAD1 OE lines correlated with increased mycorrhizal colonization. Conversely, *dad1*, *pdr1*, and *kai2a* mutants with reduced HPC density exhibited reduced mycorrhizal colonization (Kretzschmar et al., 2012) (Figure S3F). The correlation between HPC density and AM colonization indicates that HPC density may be relevant for AM symbiosis and that it can be limiting for AM. These findings also show that HPC density is an important trait in crop production because HPCs can potentially influence plant nutrition, resistance to root-borne diseases, and drought tolerance. A better understanding of the genetic basis of HPC formation will reveal how these traits are connected with endogenous developmental programs and how they can be used for crop breeding.

Limitation of the Study

The scientific interest for hypodermis differentiation is high, because of the possible implications the distribution of HPCs might have on mycorrhization and plant nutrient uptake. Still, additional studies are necessary to pinpoint the role of SL and of SL transport (via the ABCG transporter PDR1) on the identity and/or maintenance of HPCs. We discuss here the further approaches we think would allow a deeper understanding of the mechanisms behind a yet putative SL/PhKAI2a/HPC-identity regulatory pathway. AtKAI2 was shown to bind AtMAX2 in *Arabidopsis* and to perceive GR24. PhKAI2 is up-to-date the only known root-expressed KAI2 homologue in petunia. Therefore, first PhKAI2a activity as receptor of SLs, and in particular of GR24-5DS, needs to be validated *in vitro* via isothermal titration calorimetry or via yeast-2-hybrid system in combination with its putative partner PhMAX2a. An inducible system aimed to downregulate PhKAI2a might as well better serve the scope of investigating maintenance and identity, rather than the sole distribution of HPCs. An inducible system designed to knock down PhKAI2 will likely permit faster detection of changes in HPC distribution, therefore allowing one to understand how direct the influence of SL and PhKAI2 on HPC identity/maintenance is. It is tempting to speculate the presence of a direct interaction between SL synthesis via DAD1, SL reception via PhKAI2a, and HPC identity. Additional analyses on dad1xdad2 and dad1xdad2xkai2a double and triple mutants in petunia will be necessary to (1) challenge our presented model; (2) study DAD1, DAD2, and KAI2 hierarchy for regulating HPC distribution; and (3) investigate DAD2 and KAI2 either partially overlapping or distinct roles on HPC identity.

The technique used up to now to detect HPCs is based on trypan blue staining. This procedure is validated by several papers, still it does not provide any qualitative information on HPCs. The transformation of petunia with reporters (rather GUS than fluorescent due to the hypodermis strong auto-fluorescence) for genes involved in suberin metabolism, such as the ones used in *Arabidopsis* to study endodermis differentiation, will possibly help understanding the SL-driven mechanisms behind the regulation of HPC identity. Transmission Electron Microscopy might as well help quantify different suberin deposition in mutants for SL synthesis, signaling, and transport versus the WT. A parallel study on pPDR1:GUS expression patterns in SL mutants or after treatment with the hormones of this study might as well give new hints on the relation between SL transport and HPC identity.

Finally, additional physiological analyses could reveal how much plant nutrition and mycorrhization are sensitive to weak and strong changes in HPC distribution. HPC distribution was already shown to alter mycorrhization rates, but no studies investigated yet if plant nutrient uptake is affected, either with or without mycorrhization, by the number of HPCs. Root uptake of ions such as calcium was reported to be influenced by root hypodermal suberization: a wide-spectrum analysis on ion uptake in SL mutants might reveal new roles for HPC in plant nutrition.

METHODS

All methods can be found in the accompanying Transparent Methods supplemental file.

SUPPLEMENTAL INFORMATION

Supplemental Information can be found online at https://doi.org/10.1016/j.isci.2019.06.024.

ACKNOWLEDGMENTS

This work was supported by the Swiss National Science Foundation projects by the grants numbers 31003A-152831 and 31003A-169546 and the Swiss Secretariat for Education and Research and Innovation (SERI) in the frame of COST action FA1206 "STREAM."

AUTHOR CONTRIBUTIONS

G.L., L.B., and E.M. conceived experiments; G.L., M.S., C.G., S.E., S.A., and L.B. executed experiments; D.R., P.-E.C., M.V., and P.M. contributed materials. G.L., L.B., D.R., and E.M. wrote the manuscript.

DECLARATION OF INTERESTS

The authors declare no competing interest.

Received: February 24, 2019
Revised: May 19, 2019
Accepted: June 14, 2019
Published: July 26, 2019

REFERENCES

Al-Babili, S., and Bouwmeester, H.J. (2015). Strigolactones, a novel carotenoid-derived plant hormone. Annu. Rev. Plant Biol. *66*, 161–186.

Andersen, T.G., Naseer, S., Ursache, R., Wybouw, B., Smet, W., De Rybel, B., Vermeer, J.E.M., and Geldner, N. (2018). Diffusible repression of cytokinin signalling produces endodermal symmetry and passage cells. Nature *555*, 529.

Barberon, M., Vermeer, J.E., De Bellis, D., Wang, P., Naseer, S., Andersen, T.G., Humbel, B.M., Nawrath, C., Takano, J., Salt, D.E., and Geldner, N. (2016). Adaptation of root function by nutrient-induced plasticity of endodermal differentiation. Cell *164*, 447–459.

Bennett, T., Liang, Y., Seale, M., Ward, S., Müller, D., and Leyser, O. (2016). Strigolactone regulates shoot development through a core signalling pathway. Biol. Open *5*, 1806–1820.

Boher, P., Serra, O., Soler, M., Molinas, M., and Figueras, M. (2013). The potato suberin feruloyl transferase FHT which accumulates in the phellogen is induced by wounding and regulated by abscisic and salicylic acids. J. Exp. Bot. *64*, 3225–3236.

Charpentier, M., Sun, J., Wen, J., Mysore, K.S., and Oldroyd, G.E.D. (2014). Abscisic acid promotion of arbuscular mycorrhizal colonization requires a component of the PROTEIN PHOSPHATASE 2A complex. Plant Physiol. *166*, 2077–2090.

Christmann, A., Weiler, E.W., Steudle, E., and Grill, E. (2007). A hydraulic signal in root-to-shoot signalling of water shortage. Plant J. *52*, 167–174.

Conn, C.E., and Nelson, D.C. (2016). Evidence that KARRIKIN-INSENSITIVE2 (KAI2) receptors may perceive an unknown signal that is not karrikin or strigolactone. Front. Plant Sci. *6*, 1219.

Doblas, V.G., Geldner, N., and Barberon, M. (2017). The endodermis, a tightly controlled barrier for nutrients. Curr. Opin. Plant Biol. *39*, 136–143.

Drummond, R.S., Sheehan, H., Simons, J.L., Martinez-Sanchez, N.M., Turner, R.M., Putterill, J., and Snowden, K.C. (2011). The expression of petunia strigolactone pathway genes is altered as part of the endogenous developmental program. Front. Plant Sci. *2*, 115.

Enstone, D.E., Peterson, C.A., and Ma, F.S. (2002). Root endodermis and exodermis: structure, function, and responses to the environment. J. Plant Growth Regul. *21*, 335–351.

Gutjahr, C., Gobbato, E., Choi, J., Riemann, M., Johnston, M.G., Summers, W., Carbonnel, S., Mansfield, C., Yang, S.Y., Nadal, M., et al. (2015). Rice perception of symbiotic arbuscular mycorrhizal fungi requires the karrikin receptor complex. Science *350*, 1521–1524.

Hamiaux, C., Drummond, R.S., Janssen, B.J., Ledger, S.E., Cooney, J.M., Newcomb, R.D., and Snowden, K.C. (2012). DAD2 is an alpha/beta hydrolase likely to be involved in the perception of the plant branching hormone, strigolactone. Curr. Biol. *22*, 2032–2036.

Hansen, H., and Grossmann, K. (2000). Auxin-induced ethylene triggers abscisic acid biosynthesis and growth inhibition. Plant Physiol. *124*, 1437–1448.

Hayward, A., Stirnberg, P., Beveridge, C., and Leyser, O. (2009). Interactions between auxin and strigolactone in shoot branching control. Plant Physiol. *151*, 400–412.

Hose, E., Clarkson, D.T., Steudle, E., Schreiber, L., and Hartung, W. (2001). The exodermis: a variable apoplastic barrier. J. Exp. Bot. *52*, 2245–2264.

Kretzschmar, T., Kohlen, W., Sasse, J., Borghi, L., Schlegel, M., Bachelier, J.B., Reinhardt, D., Bours, R., Bouwmeester, H.J., and Martinoia, E. (2012). A petunia ABC protein controls strigolactone-dependent symbiotic signalling and branching. Nature *483*, 341–U135.

Leide, J., Hildebrandt, U., Hartung, W., Riederer, M., and Vogg, G. (2012). Abscisic acid mediates the formation of a suberized stem scar tissue in tomato fruits. New Phytol. *194*, 402–415.

Liu, G., Bollier, D., Gübeli, C., Peter, N., Arnold, P., Egli, M., and Borghi, L. (2018a). Simulated microgravity and the antagonistic influence of strigolactone on plant nutrient uptake in low nutrient conditions. NPJ Microgravity *4*, 20.

Liu, G., Pfeifer, J., de Brito Francisco, R., Emonet, A., Stirnemann, M., Gubeli, C., Hutter, O., Sasse, J., Mattheyer, C., Stelzer, E., et al. (2018b). Changes in the allocation of endogenous strigolactone improve plant biomass production on phosphate-poor soils. New Phytol. *217*, 784–798.

Liu, J., He, H., Vitali, M., Visentin, I., Charnikhova, T., Haider, I., Schubert, A., Ruyter-Spira, C., Bouwmeester, H.J., Lovisolo, C., and Cardinale, F. (2015). Osmotic stress represses strigolactone biosynthesis in *Lotus japonicus* roots: exploring the interaction between strigolactones and ABA under abiotic stress. Planta *241*, 1435–1451.

Lopez-Raez, J.A., Kohlen, W., Charnikhova, T., Mulder, P., Undas, A.K., Sergeant, M.J., Verstappen, F., Bugg, T.D.H., Thompson, A.J., Ruyter-Spira, C., and Bouwmeester, H. (2010). Does abscisic acid affect strigolactone biosynthesis? New Phytol. *187*, 343–354.

Ma, B., Yin, C.C., He, S.J., Lu, X., Zhang, W.K., Lu, T.G., Chen, S.Y., and Zhang, J.S. (2014). Ethylene-induced inhibition of root growth requires abscisic acid function in rice (*Oryza sativa* L.) seedlings. PLoS Genet. *10*, e1004701.

Martín Rodriguez, J.Á., León Morcillo, R., Vierheilig, H., Antonio Ocampo, J., Ludwig-Müller, J., and García Garrido, J.M. (2010).

Mycorrhization of the notabilis and sitiens tomato mutants in relation to abscisic acid and ethylene contents. J. Plant Physiol. *167*, 606–613.

Marzec, M. (2016). Perception and signaling of strigolactones. Front Plant Sci. *7*, 1260.

Nelson, D.C., Scaffidi, A., Dun, E.A., Waters, M.T., Flematti, G.R., Dixon, K.W., Beveridge, C.A., Ghisalberti, E.L., and Smith, S.M. (2011). F-box protein MAX2 has dual roles in karrikin and strigolactone signaling in *Arabidopsis thaliana*. Proc. Natl. Acad. Sci. U S A *108*, 8897–8902.

Parniske, M. (2008). Arbuscular mycorrhiza: the mother of plant root endosymbioses. Nat. Rev. Microbiol. *6*, 763–775.

Peterson, C.A., and Enstone, D.E. (1996). Functions of passage cells in the endodermis and exodermis of roots. Physiol. Plant. *97*, 592–598.

Rich, M.K., Schorderet, M., and Reinhardt, D. (2014). The role of the cell wall compartment in mutualistic symbioses of plants. Front. Plant Sci. *5*, 238.

Romano, C.P., Hein, M.B., and Klee, H.J. (1991). Inactivation of auxin in tobacco transformed with the indoleacetic acid-lysine synthetase gene of *Pseudomonas savastanoi*. Genes Dev. *5*, 438–446.

Sasse, J., Simon, S., Gubeli, C., Liu, G.W., Cheng, X., Friml, J., Bouwmeester, H., Martinoia, E., and Borghi, L. (2015). Asymmetric localizations of the ABC transporter PaPDR1 trace paths of directional strigolactone transport. Curr. Biol. *25*, 647–655.

Scaffidi, A., Waters, M.T., Sun, Y.K., Skelton, B.W., Dixon, K.W., Ghisalberti, E.L., Flematti, G.R., and Smith, S.M. (2014). Strigolactone hormones and their stereoisomers signal through two related receptor proteins to induce different physiological responses in *Arabidopsis*. Plant Physiol. *165*, 1221–1232.

Seto, Y., Yasui, R., Kameoka, H., Tamiru, M., Cao, M., Terauchi, R., Sakurada, A., Hirano, R., Kisugi, T., Hanada, A., et al. (2019). Strigolactone perception and deactivation by a hydrolase receptor DWARF14. Nat. Commun. *10*, 191.

Sharda, J.N., and Koide, R.T. (2008). Can hypodermal passage cell distribution limit root penetration by mycorrhizal fungi? New Phytol. *180*, 696–701.

Shishkoff, N. (1987). Distribution of the dimorphic hypodermis of roots in Angiosperm families. Ann. Bot. *60*, 1–15.

Snowden, K.C., Simkin, A.J., Janssen, B.J., Templeton, K.R., Loucas, H.M., Simons, J.L., Karunairetnam, S., Gleave, A.P., Clark, D.G., and Klee, H.J. (2005). The decreased apical dominance1/petunia hybrida CAROTENOID CLEAVAGE DIOXYGENASE8 gene affects branch production and plays a role in leaf senescence, root growth, and flower development. Plant Cell *17*, 746–759.

Steudle, E. (2000). Water uptake by roots: effects of water deficit. J. Exp. Bot. *51*, 1531–1542.

Stirnberg, P., van De Sande, K., and Leyser, H.M. (2002). MAX1 and MAX2 control shoot lateral branching in *Arabidopsis*. Development *129*, 1131–1141.

Toh, S., Holbrook-Smith, D., Stokes, M.E., Tsuchiya, Y., and McCourt, P. (2014). Detection of parasitic plant suicide germination compounds using a high-throughput *Arabidopsis* HTL/KAI2 strigolactone perception system. Chem. Biol. *21*, 988–998.

Tsuchiya, Y., and McCourt, P. (2009). Strigolactones: a new hormone with a past. Curr. Opin. Plant Biol. *12*, 556–561.

Ueda, H., and Kusaba, M. (2015). Strigolactone regulates leaf senescence in concert with ethylene in *Arabidopsis*. Plant Physiol. *169*, 138–147.

Varma Penmetsa, R., Uribe, P., Anderson, J., Lichtenzveig, J., Gish, J.-C., Nam, Y.W., Engstrom, E., Xu, K., Sckisel, G., Pereira, M., et al. (2008). The Medicago truncatula ortholog of *Arabidopsis* EIN2, sickle, is a negative regulator of symbiotic and pathogenic microbial associations. Plant J. *55*, 580–595.

Yoshida, S., Kameoka, H., Tempo, M., Akiyama, K., Umehara, M., Yamaguchi, S., Hayashi, H., Kyozuka, J., and Shirasu, K. (2012). The D3 F-box protein is a key component in host strigolactone responses essential for arbuscular mycorrhizal symbiosis. New Phytol. *196*, 1208–1216.

ISCI, Volume *17*

Supplemental Information

Strigolactones Play an Important Role in Shaping Exodermal Morphology via a KAI2-Dependent Pathway

Guowei Liu, Marina Stirnemann, Christian Gübeli, Susanne Egloff, Pierre-Emmanuel Courty, Sylvain Aubry, Michiel Vandenbussche, Patrice Morel, Didier Reinhardt, Enrico Martinoia, and Lorenzo Borghi

Supplemental figures and legends

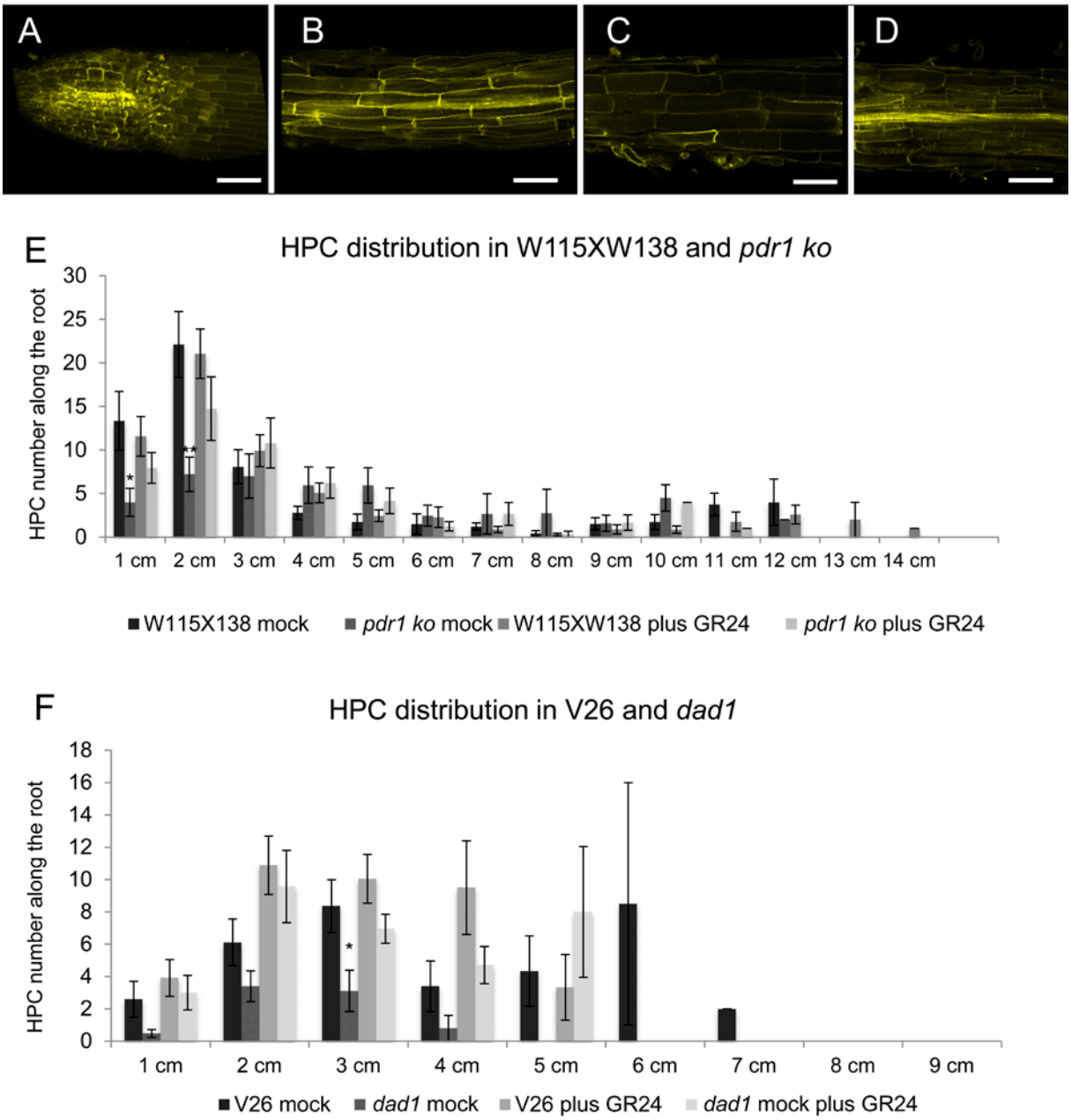

Figure S1. Related to Figure 1. Fluorol yellow staining of petunia roots and HPC distribution along the main root in *dad1*, *pdr1* and relative WT backgrounds.

(A-D) Fluorol yellow staining in root tips (a), hypodermis (b), cortex (c) and stele (d).

(E) HPC distribution in WT and *pdr1* roots, mock or 10 µM GR24 treated.

(F) HPC distribution in WT and *dad1* roots, mock or 10 µM GR24 treated.

Stars above the bars indicate statistically significant difference (T-TEST, * P ≤ 0.05, ** P ≤ 0.01). Error bars are ±SEM. Scale bars = 50 µm

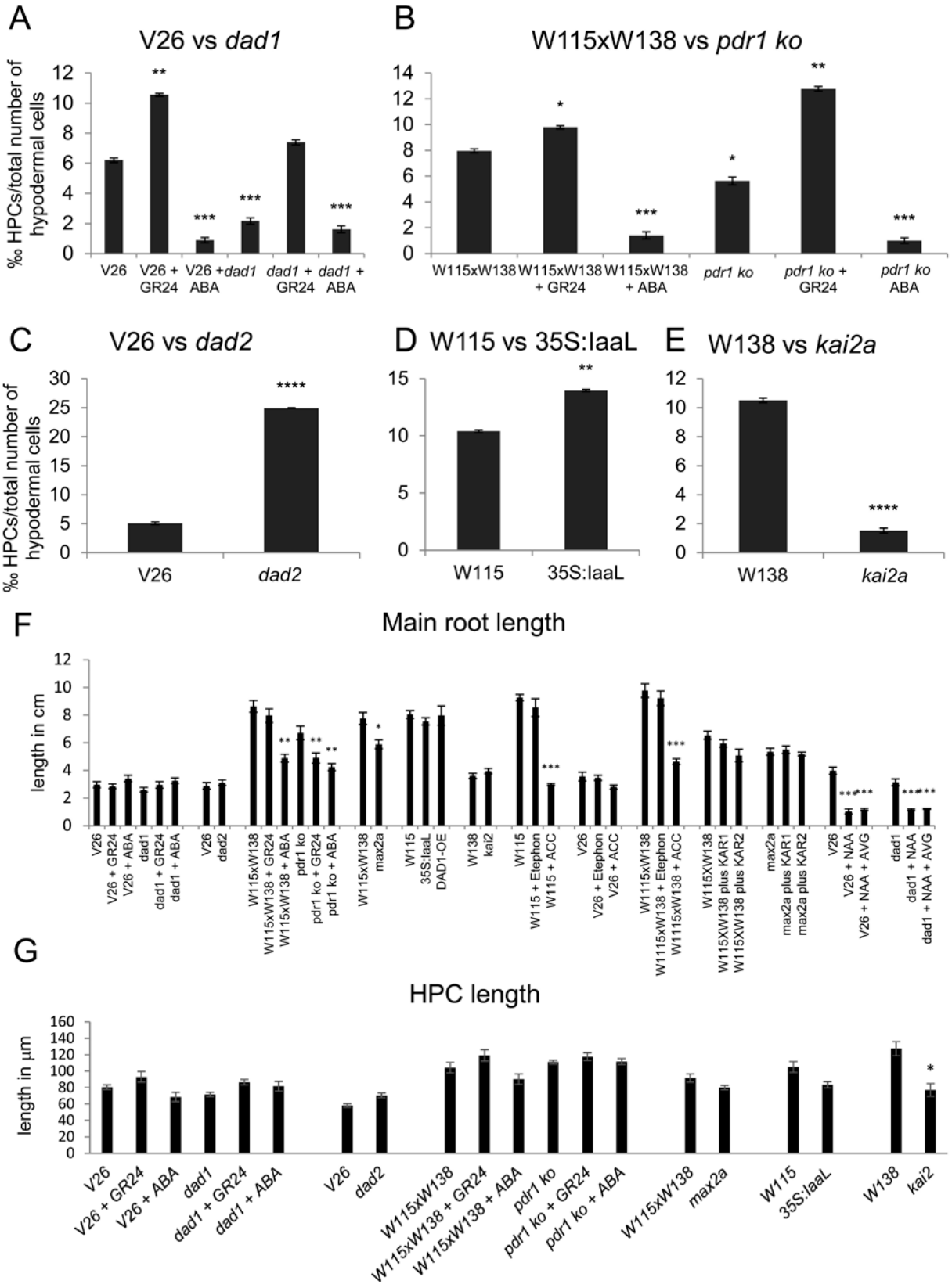
A
V26 vs dad1
‰ HPCs/total number of hypodermal cells
V26
V26 + GR24
V26 + ABA
dad1
dad1 + GR24
dad1 + ABA
B
W115xW138 vs pdr1 ko
W115xW138
W115xW138 + GR24
W115xW138 + ABA
pdr1 ko
pdr1 ko + GR24
pdr1 ko ABA
C
V26 vs dad2
‰ HPCs/total number of hypodermal cells
V26
dad2
D W115 vs 35S:IaaL
W115
35S:IaaL
E W138 vs kai2a
W138
kai2a
F
Main root length
length in cm
V26
V26 + GR24
V26 + ABA
dad1
dad1 + GR24
dad1 + ABA
V26
dad2
W115xW138
W115xW138 + GR24
W115xW138 + ABA
pdr1 ko
pdr1 ko + GR24
pdr1 ko + ABA
W115xW138
max2a
W115
35S:IaaL
DAD1-OE
W138
kai2
W115
W115 + Etephon
W115 + ACC
V26
V26 + Etephon
V26 + ACC
W1115xW138
W1115xW138 + Etephon
W1115xW138 + ACC
W115XW138
W115XW138 plus KAR1
W115XW138 plus KAR2
max2a
max2a plus KAR1
max2a plus KAR2
V26
V26 + NAA
V26 + NAA + AVG
dad1
dad1 + NAA
dad1 + NAA + AVG
G
HPC length
length in µm
V26
V26 + GR24
V26 + ABA
dad1
dad1 + GR24
dad1 + ABA
V26
dad2
W115xW138
W115xW138 + GR24
W115xW138 + ABA
pdr1 ko
pdr1 ko + GR24
pdr1 ko + ABA
W115xW138
max2a
W115
35S:IaaL
W138
kai2

Figure S2. Related to Figures 1 and 2. ‰ HPC / total number of hypodermal cells (thc), root lengths and cell lengths.

(A) ‰ HPC/thc in V26 (WT) and *dad1* roots.

(B) ‰ HPC/thc in W115xW138 (WT) and *pdr1 ko* roots.

(C) ‰ HPC/thc in V26 (WT) and *dad2* roots.

(D) ‰ HPC/thc in W115 (WT) and *35S:IaaL* roots.

(E) ‰ HPC/thc in W138 (WT) and *kai2a* roots.

(F) Main root lengths in cm.

(G) HPC cell lengths in μm.

T-TEST, * $P \leq 0.05$, ** $P \leq 0.01$, *** $P \leq 0.001$, **** $P \leq 0.0001$. Error bars are ±SEM.

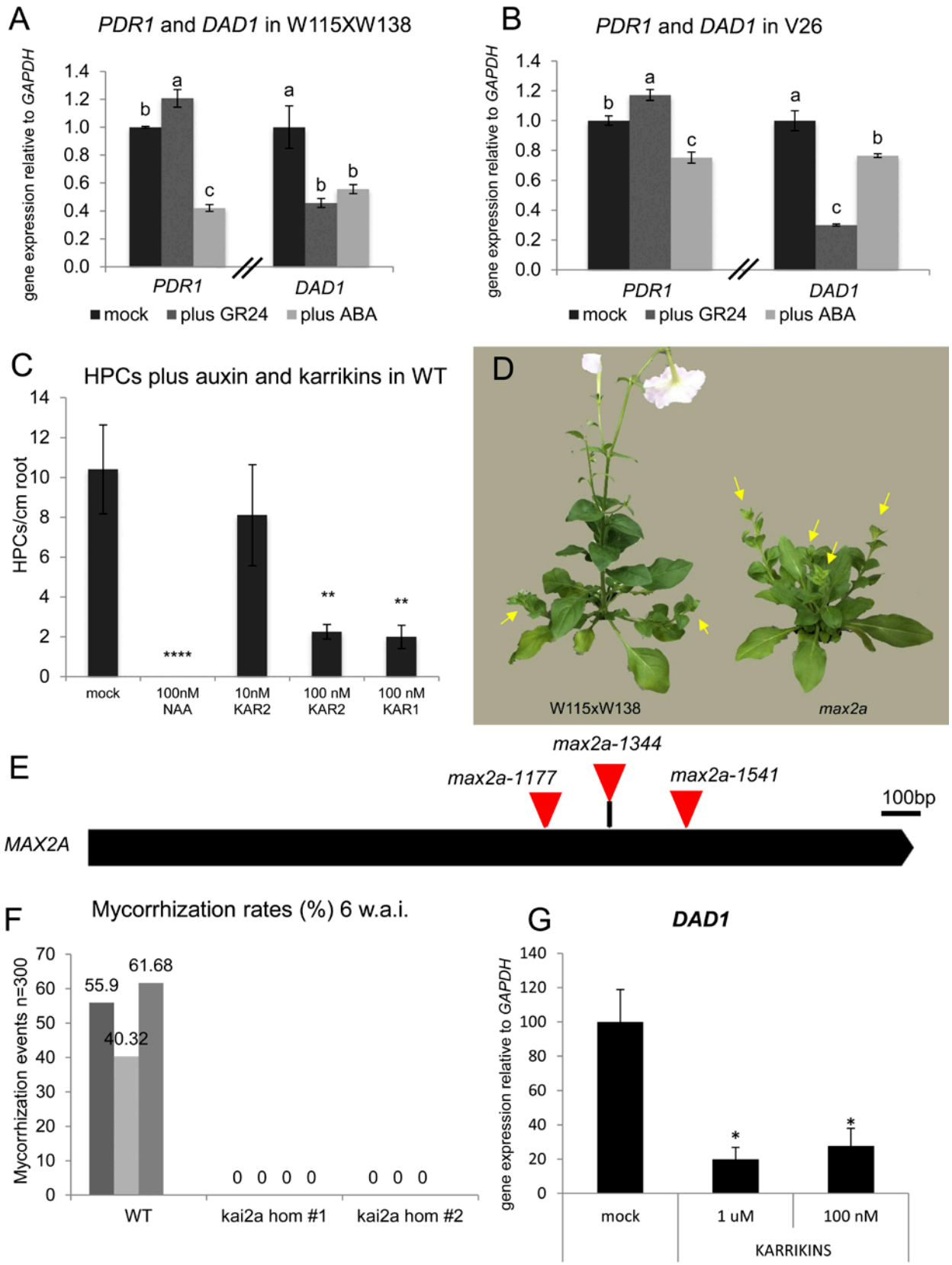
A
PDR1 and DAD1 in W115XW138
gene expression relative to GAPDH
1.4
1.2
1.0
0.8
0.6
0.4
0.2
0.0
b
a
c
a
b
b
PDR1
DAD1
mock
plus GR24
plus ABA
B
PDR1 and DAD1 in V26
gene expression relative to GAPDH
1.4
1.2
1.0
0.8
0.6
0.4
0.2
0.0
b
a
c
a
c
b
PDR1
DAD1
mock
plus GR24
plus ABA
C
HPCs plus auxin and karrikins in WT
HPCs/cm root
14
12
10
8
6
4
2
0
****
**
**
mock
100nM NAA
10nM KAR2
100 nM KAR2
100 nM KAR1
D
W115xW138
max2a
E
max2a-1344
max2a-1177
max2a-1541
100bp
MAX2A
F
Mycorrhization rates (%) 6 w.a.i.
Mycorrhization events n=300
70
60
50
40
30
20
10
0
55.9
40.32
61.68
0 0 0 0
0 0 0
WT
kai2a hom #1
kai2a hom #2
G
DAD1
gene expression relative to GAPDH
140
120
100
80
60
40
20
0
*
*
mock
1 uM
100 nM
KARRIKINS

Figure S3. Related to Figures 3 and 4. Effects of hormones on HPCs and isolation of *max2a* lines.

(A) *PDR1* and *DAD1* gene expression levels in W115xW138 plus GR24 or ABA

(B) *PDR1* and *DAD1* gene expression levels in V26 plus GR24 or ABA

(C) Effects of low levels of karrikin and auxin on HPC density.

(D) Phenotyping of *max2a* plants compared to their WT background. *max2a* mutant plants are bushy (yellow arrows = lateral branches) and dwarf

(E) Graphic representation of the insertion positions in *MAX2A*

(F) Mycorrhization rates (%) 6 weeks after inoculation (w.a.i.) in WT and *kai2a* plants.

(G) *DAD1* expression levels relative to *GAPDH* after mock, KAR1 and KAR2 1 μM or 100 nM treatments.

Different letters above the bars indicate statistically significant difference ($P < 0.05$, by one way ANOVA, $n \geq 30$). Stars above the bars indicate statistically significant difference (Student's T-test p-value < 0.05 = *; ≤ 0.01 = **; <0.0005 = ***). Error bars are ±SEM.

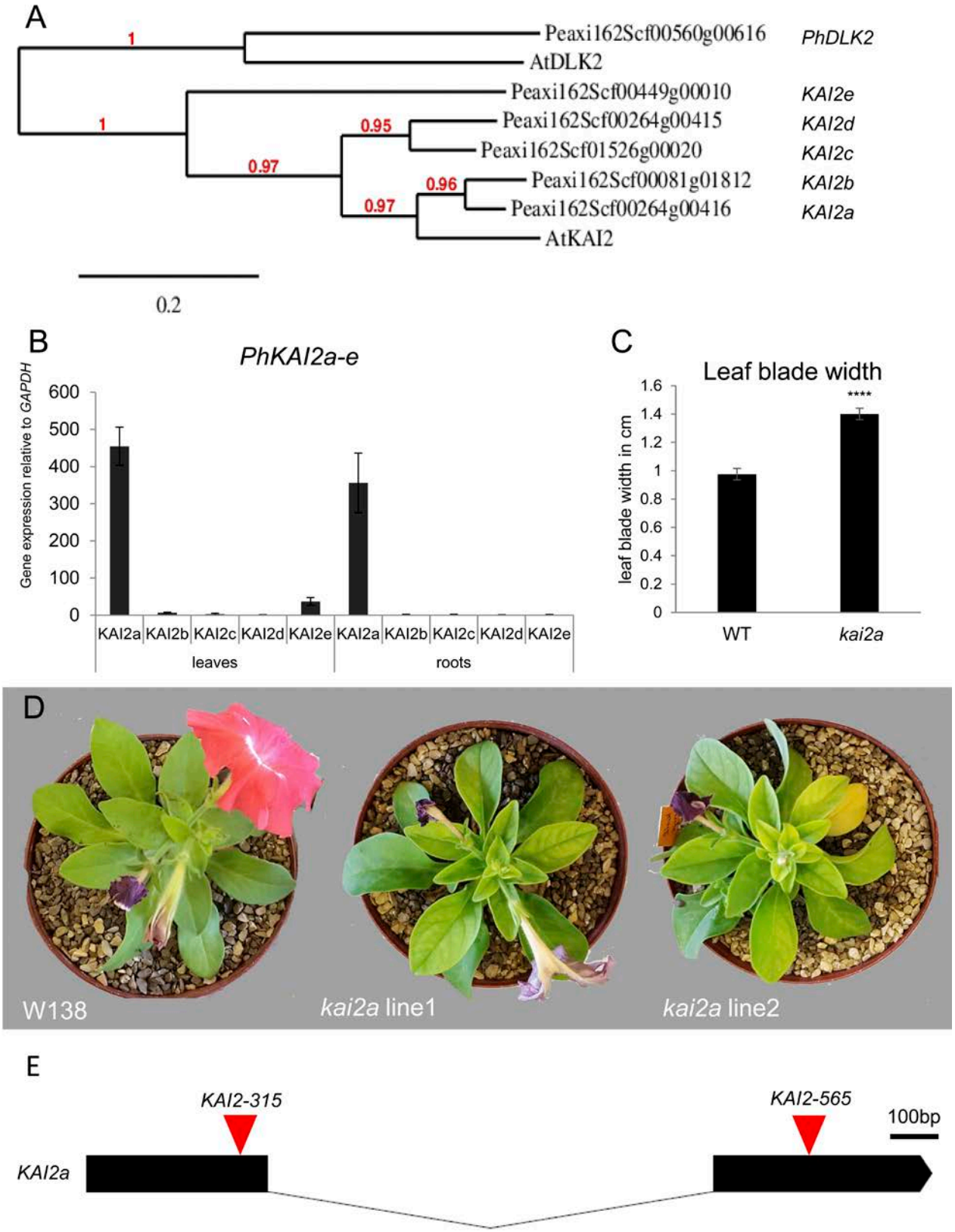
A
1
1
0.97
0.95
0.96
0.97
Peaxi162Scf00560g00616
AtDLK2
Peaxi162Scf00449g00010
Peaxi162Scf00264g00415
Peaxi162Scf01526g00020
Peaxi162Scf00081g01812
Peaxi162Scf00264g00416
AtKAI2
PhDLK2
KAI2e
KAI2d
KAI2c
KAI2b
KAI2a
0.2
B
PhKAI2a-e
Gene expression relative to GAPDH
600
500
400
300
200
100
0
KAI2a KAI2b KAI2c KAI2d KAI2e KAI2a KAI2b KAI2c KAI2d KAI2e
leaves
roots
C
Leaf blade width
leaf blade width in cm
1.6
1.4
1.2
1
0.8
0.6
0.4
0.2
0
****
WT
kai2a
D
W138
kai2a line1
kai2a line2
E
KAI2-315
KAI2-565
100bp
KAI2a

Figure S4. Related to Figures 3 and 4. Isolation of *kai2a* lines.

(A) Phylogenetic analyses (phylogeny.fr, maximum likelihood, bootstraps n = 100) of 6 *Petunia hybrida* sequences homologue to *Arabidopsis KAI2* (*AtKAI2*) and *Arabidopsis* DWARF14-LIKE2 (*AtDLK2*).

(B) Quantitative PCR analysis of *PhKAI2a-e* in leaves and roots.

(C) Leaf blade widths in WT and *kai2a* plants.

(D) Plant phenotypes of independent, 6 weeks old *kai2a* lines compared to W138 (WT).

(E) Graphic representation of the insertion positions in *KAI2a.*

Stars above the bars indicate statistically significant difference (Student's T-test p-value < 0.0005 = ***). Error bars are ±SEM.

Transparent methods

Cloning of DAD1-OE

Total RNA from mycorrhizal Petunia roots was isolated using the RNeasy Plant Mini kit (Qiagen). RNA extracts were DNase treated with the DNA-free™ Kit, DNase Treatment and Removal Reagents (AMBION® by Life Technologies). Total RNA was quantified and purity was estimated using the Nanodrop (ND-1000, Witec). Full-length doubled-stranded cDNAs were obtained using the SMART–PCR cDNA Synthesis Kit (Clontech). PCR amplification of the full-length cDNA, from the start to the stop codon, with primers designed using the nucleotide sequences was performed on a T3 thermocycler (Biometra) using the Advantage 2 Polymerase Mix (Clontech). Amplified products were cloned in the pJet1.2 vector (Thermo Fisher Scientific) and sequenced (Microsynth) by cDNA walking. PCR amplicons generated with the KAPA HiFi HotStart (Roche) were cloned into pDONR221 generating pENTR_DAD1 clones and, subsequently, cloned together with the constitutive Arabidopsis Ubiquitin10 promoter (*PUbq10*) in pDONRP4P1R and the OCS terminator (the 3′ sequences of the octopine synthase gene, including polyadenylation and presumptive transcription termination sequences) in pDONRP2RP3 into pKGW-MGW using the multiple Gateway cloning kit (Invitrogen). The pENTR clones were made by carrying out a BP-Reaction II overnight. DH5α competent cells (Invitrogen) were transformed by heat shock with 5 µl of the BP Reaction II mixture (Invitrogen). Cells were selected on LB medium with kanamycin (50 mg/ml). pENTR of positive colonies was extracted and used to perform a multiple Gateway LR cloning reaction (Invitrogen). DH5α competent cells (Invitrogen) were transformed by heat shock with 5 µl of the LR reaction mixture. Cells were selected on LB medium with spectinomycin (100 mg/ml). Colonies were

checked by PCR for the presence of the correct inserts. Expression vector of positive colonies were grown overnight in LB medium with spectinomycin (100 mg/ml) and sequences were verified by sequencing. The final expression vector was transferred to *A. tumefaciens* GV3101 through electroporation (Biorad). Positive colonies were selected after two days of growth on LB medium with spectinomycin (100 mg/ml) and tetracycline (12.5 mg/ml) overnight at 30°C.

Seedlings growth and hormonal treatments for investigation on hypodermal passage cell

Petunia hybrida lines used with W115 (Mitchell cultivar) background: W115 wild type, 35S::IAAL (Romano et al., 1991); DAD1-OE; with W115XW138 background: W115XW138 wild type, *pdr1*, *max2a*; with V26 background: V26 wild type, *dad1*, *dad2*; with W138 background: W138 wild type, *kai2*. All seeds were germinated on plates that contain 2.2 g/L MS medium (half strength Murashige and Skoog medium, Duchefa, The Netherlands) and 0.85% (w/v) Phyto Agar (Duchefa, The Netherlands) without sucrose at 21 °C, long day conditions (16 hours light / 8 hours darkness). Seedlings showing the same stage of development were transferred after 7 days to new plates for different hormonal treatments: mock, 10 µM rac-GR24 (Chiralix, The Netherlands), 100 nM to 1 µM $GR24^{5DS}$ or $GR24^{ent5DS}$ (Olchemin, Czech Republic), 1 µM ABA (Sigma-Aldrich, Switzerland), 100 nM and 1µM 1-naphthaleneacetic acid (NAA) (Sigma-Aldrich, Switzerland), 100 nM and1 µM Karrikin1 (Olchemin, Czech Republic), 10 nM, 100 nM and 1 µM Karrikin2 (Olchemin, Czech Republic), 1 µM ethephon (Sigma-Aldrich, Switzerland) or 5 µM ACC (1-aminocyclopropane-1-carboxylic acid, ethylene precursor) (Sigma-Aldrich, Switzerland), each for 3 weeks.

We experienced some efficiency variability while testing the effects of racemic mixtures of GR24 and its single enantiomers, $GR24^{5DS}$ and $GR24^{ent\text{-}5DS}$ on HPC abundances. For example, 10 µM *rac-GR24* was sufficient to recover HPC abundances in *dad1* mutants, while 1 µM of the single enantiomer $GR24^{5DS}$ could only double the HPC numbers in *dad1* and 100 nM had no effects. We hypothesize that different levels of purity of the two compounds, or different from 1:1 expected ratio of the enantiomers in *rac-GR24* might be responsible for the different efficiencies of the recovery.

Trypan blue staining of HPCs and mycorrhization quantification

Trypan blue was chosen to stain HPCs instead of fluorol yellow (the method of choice for endodermal cells) because it gives the possibility of easily detecting a dark stained cell surrounded by transparent epidermal and cortex cells (Figure 1A-I). The fluorol yellow would stain instead all cell walls of the hypodermis with the exception of HPC, which are additionally

strongly auto fluorescent as previously reported in *Petunia* (Figure S1A-D) (Sasse et al., 2015) making it possible to recognize HPCs in single radial sections only and not, as required for this study, along the whole root length, where (longitudinal) sections would anyway not allow to follow the undulated root morphology. Roots of plate-grown plantlets were carefully separated from the gel and directly incubated for 1 min in 5% HCl. The acidified roots were stained for 2.5 h in trypan blue solution (2.5% glacial acetic acid; 47.5% ddH_2O; 50% glycerol; 0.6 g/L trypan blue). Afterwards, 5% acetic acid was used to wash and de-stain the roots overnight. The HPCs were counted under a binocular microscope. All HPCs from whole root (above the fully stained blue root tip) were calculated segment by segment of 1 cm each. The HPCs densities were showed as total HPCs number divided by total root length. The *HPC/total number of hypodermal cells (thc) per thousand* (‰) was calculated as the ratio between the total number of HPCs divided by the estimated total number of thc (the latter was calculated by the ratio of seedling root length / HPC length, this ratio then multiplied by 8, which is the average number of hypodermal cells around the stele in the different genotype/treatments). HPC lengths were quantified per genotype/treatment, n=15 per genotype/treatment.

Mycorrhization quantification as reported in (Kretzschmar et al., 2012) with no changes. In short, 5 to 8 biological replicates, 200 to 500 grid-root intersections each, were quantified for either the presence or absence of mycorrhization or specific mycorrhizal structure, i.e. vesicles, intraradical hyphae and arbuscules.

Fluorol yellow staining protocol was applied with no changes as reported in the website of Geldner's group: wp.unil.ch/geldnerlab/files/2013/07/Fluorol-Yellow-staining.pdf

Petunia transformation

A bacterial suspension (pre-culture) was prepared from a 100 µL frozen glycerol culture in 5 mL of LB medium (10 g/l bacto-tryptone, 5 g/l bacto-yeast extract, 10 g/l NaCl, pH 7.5) supplemented with 50 mg/l kanamycin and 25 mg/l rifampicin and cultured overnight at 28 °C with shaking (250 rpm). Then 200µl of the pre-culture was added to 50 ml of LB medium supplemented with 50 mg/l kanamycin and 25 mg/l rifampicin and cultured for about 6h at 28 °C with shaking (250 rpm). The bacterial suspension with an OD600 = 0.6 was pelleted at 4,000 rpm for 15 min at 4 °C. The supernatant was discarded, and the pellet was re-suspended in 50 mL of half strength liquid MS medium supplemented with 150 µM acetosyringone.

Young Petunia leaves were harvested from growth chamber-grown plants, surface sterilised by soaking in 2 % (w/v) sodium hypochlorite with 0.1 % Tween 20 for 15 min, and subsequently

rinsed three times in sterile water. Young leaf explants were cut through the midrib to obtain 10 x 20 mmm rectangular explants (50-60 pieces) and submerged in the bacterial solution for 10 min.

The Petunia explants were blotted dry on sterile filter paper and placed on co-cultivation media for 2 days: 2.2 g/l Murashige and Skoog (MS) medium supplemented with 20 g/l sucrose, 10 g/l glucose, 8 g/l plant agar (Duchefa). The pH was adjusted to 5.7 before autoclaving and 15 mg/l (75µM) acetosyringone is added after autoclaving.

After co-cultivation, in vitro shoot regeneration of the explants was performed on 10 cm diameter Petri dishes containing the shoot-inducing media (pH adjusted to 5.7 before autoclaving), that is a solid regeneration medium based on half strength MS medium (2.2 g/l) supplemented with 20 g/l sucrose, 10 g/l glucose, 8 g/l plant agar (Duchefa). After autoclaving and before pouring, the media was supplemented with MS vitamins, 500 mg/l cefotaxime, 300 mg/1 kanamycin, 2 mg/l 6-benzylaminopurin (BAP) and 0.2 mg/l 1-naphthaleneacetic acid (NAA). The explants were transferred into fresh media every 3 weeks. Once appeared, regenerated shoots were cut from the explant and transferred to a root-inducing MS medium containing half MS medium plus MS vitamins, hormone-free containing 500 mg/1 cefotaxime and 100 mg/1 kanamycin. The shoots were transferred into fresh media every 3 weeks until they were 4 to 8 cm high and produced a well-developed root system. Then, the plants were acclimatized and transferred to growth chamber conditions. Shoot regeneration and root induction were performed in a growth chamber at 24 °C with a 16 h photoperiod of 32 µmol m^{-2} s^{-1} illumination.

Free auxin quantification

Hormonal characterization in *Petunia* samples was a service performed by the Institute of Experimental Botany CAS, Prague (Czech Republic). Samples were freeze-dried, shipped and analyzed as previously reported (Dobrev and Vankova, 2012; Djilianov et al., 2013). Hormonal profiling was quantified on fresh and dry weight.

Quantitative PCR

RNA was extracted from petunia roots using the RNeasy Plant Mini Kit (Qiagen, Switzerland). Reverse transcription to cDNA was performed with M-MLV reverse transcriptase, RNase H minus, point Mutant (Promega, Switzerland) and oligo dT primers (Promega, Switzerland). *PhGAPDH* served as housekeeping gene (Kretzschmar et al., 2012; Sasse et al., 2015). The primer sequences used to quantify *PDR1* and *MAX1* expression are given in (Kretzschmar et al., 2012; Sasse et al., 2015). For *DAD1* expression, the primers used were 5’ -GGC AAA ATT GTG GCA AGT GTA- 3’ and 5’ -ATC TCC CAA CCC TTG CAT CC- 3’. SYBR green PCR Master Mix

(Applied Biosystems) was used for quantitative PCR with a 7500 Fast Real Time PCR system (Applied Biosystem). Three biological replicates were performed for each experiment. For each single replicate, 30-40 seedlings were pooled for RNA extraction. The primers used to quantify gene expression of *KAI2a-e* follow (forward; reverse): PaKAI2a (TCTCCAAGGTACCTGAACGA; CTACCGAGTCCATGTCACCT); PaKAI2b (TATGTTGGTCACTCTGTTTCTGCT; CATTCAAGAACCTGGGAGAAGCAC); PaKAI2c (CTTCTCCAAGGTTCATAAATGCAG, GCCACTGAATCCATGTCACC); PaKAI2d (TTTCTGTCCCAAGTTACTGTGCC; CTTTGTTTCCATCTCACTGCCTC); PaKAI2e (GCATTTATGTTGGTCACTCTGTC; CATGTCATTCAGATACCTGGGAG); PaDLK2-like (TTCTCCCAGGTTCATAAATTCGGA; CCTGTACTCCACACGTCATAGTC)

Petunia kai2a and max2a mutant genotyping

Petunia *kai2a* and *max2a* mutants were identified by searching a sequence-indexed dTph1 transposon database (Vandenbussche et al., 2008), which has been considerably expanded in recent years. All identified mutant alleles are *dTph1* insertions in the coding sequence (Figure S3E, S4E), and are likely to disrupt gene function because the 284bp dTph1 element contains multiple stop codons in all six possible reading frames. Exact insert positions (expressed in base pairs downstream of the ATG start codon with the coding sequence as a reference) were determined by aligning the *dTph1* flanking sequences with the genomic and cDNA sequences. All in silico-identified candidate insertions were confirmed by PCR-based genotyping of the progeny from the selected insertion lines, using primers flanking the *dTph1* transposon insertions. The following thermal profile was used for segregation analysis PCR: 10 cycles (94°C for 15 s, 68°C for 20 s minus 1°C/cycle, 72°C for 30 s), followed by 40 cycles (94°C for 15 s, 58°C for 20 s, and 72°C for 30 s). The different insertion mutants were further systematically genotyped in subsequent crosses and segregation analyses. PCR products were analyzed by agarose gel electrophoresis. The primers used to identify homozygote plants follow (forward; reverse): KAI2-315 (TTGGACATTCTGTTTCTGCCATG; GAACCAGAGACGGTGACAAG); KAI2-565 (TTCAACATGAGACCAGACATAGC; ATGAGGCAACAAATGTCTTAAATCAC); MAX2A-1177(CAAGTTTGAGGTCCAAGGTTG; GCTCCAAGATTCTTGCAGCA); MAX2A-1344 (TTGATTGTGTGTGGGATAGTG; TGCTTGAAGCTTCACATCCAT); MAX2A-1541 (GGCAATGGATATAGTGGACG; GTCTTCAAGACCTGCAGCTG).

Statistical analyses

Experiments were repeated a minimum of three times (three biological replicates). For each biological replicate, 30-40 seedlings were collected for qPCR analyses; 8-15 roots per line per

treatment were analyzed for HPC numbers. The sample size was chosen accordingly to the equally distributed and stable growth conditions in our greenhouse, as well as to the homogeneity of our already published transgenic lines. In the case *kai2* transgenic lines, we quantified morphology and phenotype in 2 independent lines to avoid insertion position effects. No samples were excluded, no criteria were pre-established. The locations of plants in the greenhouse were randomized to avoid any position effect. Blinding was applied in quantifying HPCs. Statistical tests, one-way Anova or Students's T-test (two-sided), are justified as appropriate because of the chosen sample size and the assumed normal distribution of samples, the latter confirmed by the data collected.

Supplemental References

Djilianov, D.L., Dobrev, P.I., Moyankova, D.P., Vankova, R., Georgieva, D.T., Gajdošová, S., and Motyka, V. (2013). Dynamics of Endogenous Phytohormones during Desiccation and Recovery of the Resurrection Plant Species Haberlea rhodopensis. J Plant Growth Regul 32, 564-574.

Dobrev, P.I., and Vankova, R. (2012). Quantification of Abscisic Acid, Cytokinin, and Auxin Content in Salt-Stressed Plant Tissues. In Plant Salt Tolerance: Methods and Protocols, S. Shabala and T.A. Cuin, eds (Totowa, NJ: Humana Press), pp. 251-261.

Romano, C.P., Hein, M.B., and Klee, H.J. (1991). Inactivation of auxin in tobacco transformed with the indoleacetic acid-lysine synthetase gene of Pseudomonas savastanoi. Genes Dev 5, 438-446.

Vandenbussche, M., Janssen, A., Zethof, J., van Orsouw, N., Peters, J., van Eijk, M.J.T., Rijpkema, A.S., Schneiders, H., Santhanam, P., de Been, M., van Tunen, A., and Gerats, T. (2008). Generation of a 3D indexed Petunia insertion database for reverse genetics. Plant Journal 54, 1105-1114.